Full Paper

Propellants, Explosives, Pyrotechnics

DOI: 10.1002/prep.201700150

Detonation Performance Characterization of a Novel CL-20 Cocrystal Using Microwave Interferometry

Vasant S. Vuppuluri,*[a] Philip J. Samuels,[b] Kelley C. Caflin,[b] I. Emre Gunduz,[a] and Steven F. Son[a]

In Honor of Dr. Michael Hiskey

Abstract: Development of novel energetic materials is a significant challenge. Cocrystallization has been explored as another route to development of novel materials. However, very little characterization of detonation performance has been performed for these energetic cocrystals. A major challenge for performing detonation velocity measurements with cocrystals is that typical measurement techniques require hundreds of grams to kilograms of material, an amount that exceeds the entire supply of many cocrystals. In this work, small-scale detonation velocity measurements using about 1.2 g of material per test employing microwave interferometry are presented and discussed for a novel cocrystal of 1-methyl-3,5-dinitro-1,2,4-triazole (MDNT) and hexanitrohexaazaisowurtzitane (CL-20) in a 1:1 molar ratio and compared to a physical mixture of MDNT and CL-20 in the same molar ratio. The results are compared with detonation velocity measurements with cyclotetramethylene tetranitramine (HMX), which provide validation of the technique and further comparison of the results. With this technique, detonation velocity differences as low as 100 m/s are resolvable. The MDNT/CL-20 cocrystal is observed to detonate over 500 m/s faster than the physical mix and over 600 m/s faster than HMX at the same charge density which is held constant in this work. The enthalpy of formation of the MDNT/CL-20 cocrystal was also measured. Using this, the detonation velocity of the cocrystal was calculated using thermochemistry to be 230 m/s faster than that of the physical mixture of MDNT and CL-20 in the same molar ratio as is contained within the cocrystal at a charge density of 1.4 g/cm^3. The higher detonation velocity of the cocrystal (both measured and predicted) compared to the physical mixture is likely attributable to bonding energy contained within the cocrystal and the arrangement of the coformers within the cocrystal.

Keywords: cocrystal · detonation · microwave interferometry

1 Introduction

Similar to drug discovery, development of novel energetic molecules is a significant challenge. A thorough characterization of the sensitivity and stability of the material must then be performed. The detonation performance of the material must then be characterized in order to evaluate the justification for scale-up. However, it is very costly to make sufficient material so small-scale characterization is needed.

Cocrystallization offers a new route to the development of novel explosive materials. A cocrystal is a combination of two crystalline materials resulting in a new material with a unique crystal structure and material properties. Cocrystallization has been of interest to the pharmaceutical industry because of its potential as a new route to drug discovery [1]. Cocrystallization offers the potential to develop novel materials with potentially attractive properties using existing materials, even ones that were previously rejected for reasons such as high sensitivity. Cocrystal explosives could have higher densities and improved morphologies, leading to improved performance and sensitivity. It is also possible that the energetics of the cocrystal could change, affecting its performance.

The first synthesis of a hexanitrohexaazaisowurtzitane (CL-20) cocrystal was reported in 2011 with trinitrotoluene (TNT) as the coformer and it was reported that the cocrystal was less sensitive than CL-20 [2]. In 2012, a cocrystal of CL-20 with HMX in a 2:1 molar ratio, was reported [3]. At its theoretical maximum density (TMD), this cocrystal was predicted to have a detonation velocity that was 100 m/s greater than that of all polymorphs of HMX at their respective crystal densities [3]. Furthermore, the CL-20/HMX 2:1 cocrystal was found to be as sensitive as HMX, which itself is less sensitive than CL-20 [3]. An open question, however, is whether a cocrystal will display measurably different

[a] *V. S. Vuppuluri, I. E. Gunduz, S. F. Son*
Department of Mechanical Engineering
Purdue University
585 Purdue Mall
West Lafayette, IN 47907 USA
**e-mail: vvuppulu@purdue.edu*
[b] *P. J. Samuels, K. C. Caflin*
US Army Armament Research Development and Engineering Center (ARDEC)
Explosives Research Branch, Building 3028
Picatinny Arsenal, NJ 07806, USA

detonation performance compared to a physical mixture of the coformers in the same molar ratio as contained in the cocrystal.

As part of a study to replace TNT in melt-cast explosive formulations, 1-methyl-3,5-dinitro-1,2,4-triazole (MDNT) was identified as a potential candidate for this purpose [4]. Similar to TNT, it has a stable melt phase [5]. This material was recently used as a coformer with CL-20 for the synthesis of a cocrystal in a 1:1 molar ratio [5]. It was produced in several gram quantities using a resonant acoustic method previously used to produce similar quantities of the CL-20/HMX 2:1 cocrystal [6]. The cocrystal was found to be less sensitive to impact than CL-20 but remained as sensitive to friction and electrostatic dis- charge as CL-20 [5].

Microwave interferometry (MI) is a well-established technique for measuring detonation velocity. The fringe pattern characteristic of interferometer systems results from an advancement in phase of the reflected microwaves relative to the incident microwaves. In a detonating explosive, the detonation front acts as a dielectric discontinuity. The microwaves reflecting on this moving surface, as well as ions from reactions, have a continuously advancing phase relative to the incident signal. This technique was used by Cawsey et al. to measure the detonation velocity of an explosive charge [7]. The underlying principle of microwave interferometry is reflectivity of the shockwave to microwaves. It has been demonstrated using inert materials that the density discontinuity at a shock front is adequate reflection of microwaves [8]. It was shown in similar experiments with reactive materials that ions from the chemical reactions further contribute to microwave reflections [9]. This technique has also been used to study deflagration-to-detonation and shock-to-detonation processes in explosives [10, 11].

The detonation velocity can then be calculated from the equation

$$U = \frac{\lambda_g}{2} f \tag{1}$$

where U is the detonation velocity, λ_g is the interference wavelength and f is the frequency. The interference wavelength λ_g is found from the equation

$$\lambda_g = \frac{\lambda_0}{\sqrt{\varepsilon_r - (\lambda_0/\lambda_c)^2}}, \tag{2}$$

where λ_0 is the free-space wavelength, λ_c is the cutoff wavelength, and ε_r is the relative permittivity of the material [7]. The cutoff wavelength λ_c is defined as the minimum wavelength below which electromagnetic waves will not propagate within the confiner, which is given by the expression $\lambda_c = 3.413R$ for a circular geometry, where R is the radius of the confiner [7]. The Landau-Lifshitz/Looyenge relation gives the permittivity for a mixture as

$$\varepsilon_r^{1/3} = (\varepsilon_A^{1/3} - \varepsilon_B^{1/3}) V_A + \varepsilon_B^{1/3}, \tag{3}$$

where ε_A and ε_B are the relative permittivities of material A and B respectively and V_A is the volume fraction occupied by material A. Taking the explosive material to be material A and air to be material B ($\varepsilon_r = 1$ for air), Eq. (3) simplifies to

$$\varepsilon_r^{1/3} = (\varepsilon_{r,TMD}^{1/3} - 1) \frac{\rho_0}{\rho_{TMD}} + 1, \tag{4}$$

where ρ_0 is the charge or powder density and the ρ_{TMD} is the theoretical maximum density (TMD) of the explosive.

The objective of this study is to determine the contribution of coformer bonding to detonation performance by quantifying the difference in detonation velocity of a cocrystal and physical mixture. To accomplish this, a small-scale detonation experiment was developed.

2 Experimental Section

2.1 Sample Preparation

An uncertainty analysis of detonation velocity revealed that charge diameter uncertainty has the most impact on the uncertainty in charge density and consequently overall uncertainty in detonation velocity. To minimize the uncertainty in diameter, precision ground stainless steel tubes from McMasterCarr (6100K148) having an inner diameter of 6.52 mm and wall thickness of 0.71 mm were used. These tubes were measured using gage pins accurate to 25 μm. The confiners were machined to a height of 57.15 ± 0.025 mm. In order to initiate the cocrystal quickly to a steady detonation velocity, the booster charge that was 25.4 mm in height consisting of HMX, Grade B, Class 3 was pressed first. The booster was pressed in two increments with 12.7 mm aluminum spacers machined to a tolerance of 25.4 μm used to obtain a consistent booster charge height. The booster charge was pressed to a density of 85 percent TMD. A piece of 25 μm aluminum foil was then pressed into the confiner to ensure that the start of the sample detonation could be seen clearly in the microwave interferometer signal. The sample charge was pressed in six increments in order to minimize density gradients [12, 13]. The height of each booster increment was kept constant using aluminum spacers machined to a height of 4.24 ± 0.025 mm. All test samples were pressed to a nominal density of 1.4 g/cm^3 in order to compare detonation speeds for the three materials at a fixed charge density. No binder was used to press either the booster or sample charge.

The MDNT/CL-20 cocrystal was prepared using the resonant acoustic mixing method [5]. The physical mixture of MDNT and CL-20 was prepared in the same molar ratio as was in the cocrystal. A batch of about 5 g of MDNT/CL-20 1:1 physical mixture was prepared in order to have enough material for four detonation measurements. To prepare this

batch, 3.698 g (8.44×10^{-3} mol) of CL-20 and 1.464 g (8.46×10^{-3} mol) of MDNT were mixed thoroughly using a roller mill.

2.2 Detonation Experiment

A diagram of the detonation experiment is shown in Figure 1. The charge is initiated with a Teledyne RISI RP-502 exploding bridgewire (EBW) detonator. A fiber optic cable is inserted at the junction between the detonator and charge to act as a trigger for the oscilloscope. A piece of 6.35 mm PTFE rod serving as the waveguide is inserted into the sample end and secured with tape. This assembly is placed inside a fragment box. The other end of the PTFE waveguide is inserted into a port on the custom-built 35 GHz microwave interferometer [12,14]. Triple-shielded cables (Pasternack PE–P195) were used to connect the two channels from the MI to the first two channels on a Tektronix DPO4034 oscilloscope. The fiber optic cable is connected to a Thorlabs DET10A detector, which was connected to the third channel on the oscilloscope such that the light from the detonator would trigger the oscilloscope. The oscilloscope records a trace for 200 μs.

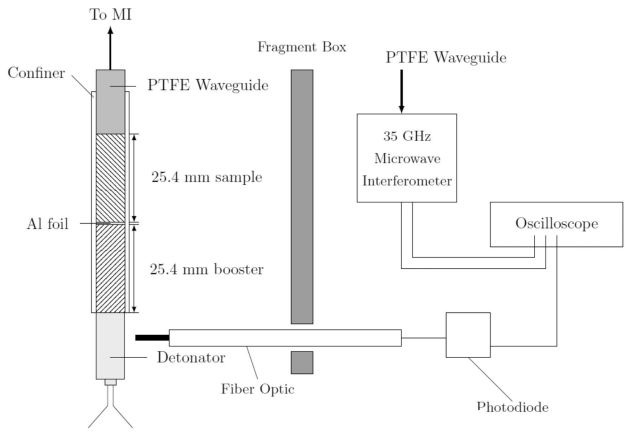

Figure 1. Diagram of detonation experiment.

2.3 Analysis Methods

A portion of the microwave interferometer raw data from a typical detonation test is shown in Figure 2. The second waveform in Figure 2 denoted by CH2 is the quadrature signal, which has a 90° phase offset from the first channel. An initial estimate of the start and end time of the detonation event is made from the waveform. The portion of each waveform that is within this time range is selected. A Butterworth second-order low-pass filter is applied to minimize noise from the two signals, after which the waveforms are

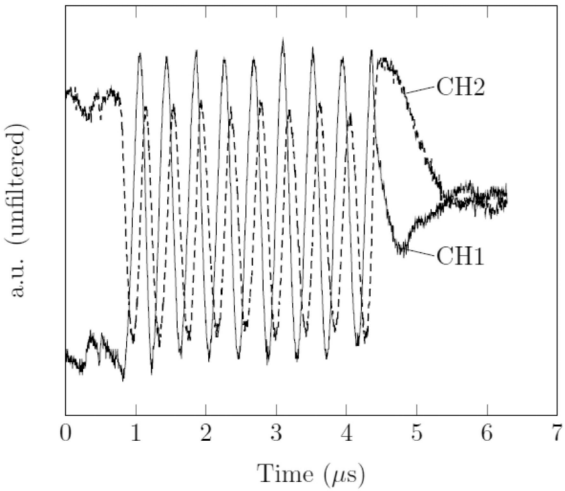

Figure 2. Unfiltered data from microwave interferometer.

normalized such that the amplitudes lie between [−1,1]. The two waveforms are then fit to the function

$$g(t) = a\sin(2\pi ft + \phi) + c, \tag{5}$$

where a is the amplitude, f is the frequency, φ is the phase offset, and c is the signal offset. The Gauss-Newton algorithm is employed to determine the constants shown in Eq. (5). This curve-fit is also used to obtain an accurate estimate of the start and end time of the detonation event. Clean waveforms were obtained for all the tests presented in study making them amenable to peak-picking. However, the quadrature method was used in order to improve spatial resolution [15]. The instantaneous phase is calculated as

$$\phi(t) = \tan^{-1}\left(\frac{V_2}{V_1}\right), \tag{6}$$

where V_2 and V_1 are the filtered and normalized waveforms. A phase unwrapping algorithm is then applied to this data to yield the instantaneous phase. From the instantaneous phase, the detonation velocity is defined as [14].

$$v(t) = \frac{\lambda_g}{4\pi}\frac{d\phi}{dt}, \tag{7}$$

Defining v(t) in Eq. (7) as *dx/dt* and integrating both sides over the entire waveform yields position as a function of time given as

$$x(t) = \frac{\lambda_g}{4\pi}\phi(t). \tag{8}$$

Knowing the length of the charge and the total phase, the dynamic interference wavelength is obtained by solving Eq. (8) for λ_g. Either the wavelength obtained from meas-

ured permittivity or that obtained from the detonation experiment itself is then substituted in to Eq. (8) to construct a position-time plot.

3 Results and Discussion

3.1 Uncertainty Quantification

Random error and bias error are the two components of overall experimental error. The uncertainty of this measurement technique was computed in order to obtain an understanding of the resolution possible with this experiment. Given a measured quantity W as a function of input parameters $X_i \ldots X_n$, the measurement uncertainty is defined as

$$\frac{\Delta W}{W} = \sqrt{\sum_{i=0}^{n} \left(\frac{\partial W}{\partial X_i} \frac{\Delta X_i}{W} \right)^2}. \tag{9}$$

In this case, it is desired to find the uncertainty in the detonation velocity. Given the equation for detonation velocity, the uncertainty in detonation velocity is given by

$$\frac{\Delta D}{D} = \sqrt{\left(\frac{\Delta \lambda_g}{\lambda_g} \right)^2 + \left(\frac{\Delta \bar{f}}{\bar{f}} \right)^2}. \tag{10}$$

The uncertainty in the material wavelength is

$$\frac{\Delta \lambda_g}{\lambda_g} = \sqrt{\left(\left(\frac{\lambda_g}{\lambda_c} \right)^2 \frac{\Delta \lambda_c}{\lambda_c} \right)^2 + \left(\left(\frac{\lambda_g}{\lambda_0} \right)^2 \frac{\Delta \varepsilon_r}{2} \right)^2}. \tag{11}$$

Knowing that $\lambda_c = 3.413R$, $\Delta\lambda_c/\lambda_c = \Delta d/d$. The term $\Delta\varepsilon_r$ is given as

$$\Delta \varepsilon_r = \sqrt{a^2 + b^2}, \tag{12}$$

where

$$a = 3\left(\varepsilon_r^{1/3} - 1\right)\varepsilon_r^{2/3} \frac{\Delta \rho_0}{\rho_0} \tag{13}$$

and

$$b = \varepsilon_r^{2/3} \left[\left(\varepsilon_r^{1/3} - 1\right) \frac{\rho_{TMD}}{\rho_0} + 1 \right]^{-2} \Delta \varepsilon_{r,TMD}. \tag{14}$$

The uncertainty in charge density denoted by $\Delta\rho_0/\rho_0$ is

$$\frac{\Delta \rho_0}{\rho_0} = \sqrt{\left(\frac{\Delta L}{L} \right)^2 + \left(2\frac{\Delta d}{d} \right)^2 + \left(\frac{\Delta m}{m} \right)^2}. \tag{15}$$

The measurement uncertainty was computed for a nominal charge density of 1.4 g/cm^3. The uncertainty in charge length ΔL was taken to be 25.4 μm. The spacers were measured to be 25.5 mm with micrometer that is accurate to ±0.51 μm. The uncertainty in the mass measurement m is twice the manufacturer's stated uncertainty of 3.1 mg. The uncertainty in the diameter d is taken to be 25.4 μm, which is the accuracy of the gage pins used to measure the diameter of the confiners. The uncertainty in the density-corrected permittivity $\varepsilon_{r,TMD}$ is 0.05 [16]. Using Equations 10 through 15, the uncertainty in the detonation velocity was found to be 1.68 percent. For a detonation speed of about 7 km/s, this results in an uncertainty of 118 m/s.

3.2 Experimental Method Validation

To demonstrate the validity of the sample preparation and measurement technique, repeated detonation tests with HMX, Grade B Class 3 were conducted. The HMX detonation tests were also used to validate the approach for determining material wavelength from the test. Using measured permittivity, position-time plots were obtained for HMX using Eq. (8) and are shown in Figure 3. For the first detonation test with HMX, a Butterworth second-order high-pass filter was applied as an additional step in the postprocessing. This step was not applied with any other HMX detonation tests. It was expected that there would be unsteady effects immediately following the detonation wave propagating into the sample. However, it is evident from Figure 3 that these unsteady effects are below the resolution of the measurement technique. This indicates that the booster charge was chosen appropriately to approximately match the resulting shockwave in the test material. A linear curve fit was applied to each of the position-time plots obtained from the HMX detonation tests in order to determine the detonation velocity for each sample.

The results are summarized in Table 1, in which ρ_0 represents the charge density, $\lambda_g^{(M)}$ represents measured wavelength, and $\lambda_g^{(D)}$ represents dynamic wavelength. The rela-

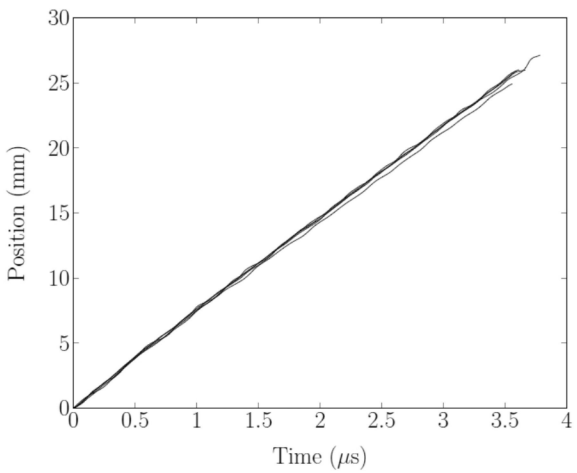

Figure 3. Position vs. time plots of HMX detonation tests.

Table 1. Wavelengths and densities for HMX detonation tests.

Shot	ρ_0 (g/cm^3)	$\lambda_g^{(M)}$ (mm)	$\lambda_g^{(D)}$ (mm)
1	1.377	6.05	5.68
2	1.406	5.98	5.88
3	1.414	5.96	5.85
4	1.413	5.96	5.85
5	1.416	5.96	5.84

tive standard deviations for the measured wavelength and dynamic wavelength are 0.62 and 1.36 percent, respectively. The dynamic wavelength is an average of 2.66 percent lower than the measured wavelength. As noted previously, the dynamic wavelength is determined by selecting the portion of the waveform that includes the estimated start and end time of the detonation event. After calculating the instantaneous phase, Eq. (8) is then solved for λ_g using the charge length and total phase. The total phase is sensitive to uncertainty in selecting the start and end time of the detonation event. The observed difference between measured and dynamic wavelength is therefore attributable to propagated error in the estimated start and end time of the detonation event. Detonation velocities were obtained for five HMX tests using the measured wavelength. Similar calculations were performed using the dynamic wavelength. The measured detonation velocities were then compared to the detonation velocity predicted CHEETAH using the JCZ3 equation of state. The results are shown in Table 2. From the detonation velocities shown in Table 2, the average detonation velocity using measured permittivity obtained for HMX is 7.15 km/s with a standard deviation of 40 m/s. This is 2.9 percent lower than the predicted velocity of 7.36 km/s, which is expected because CHEETAH assumes an infinitesimal reaction zone. Using CHEETAH, a relationship between charge density and detonation velocity was found to be of the form

Table 2. Measured HMX detonation velocities.

Shot	ρ_0 (g/cm^3)	U (km/s) (Est.)	(Meas.)	(Meas., dyn.)	(CHEETAH)	(Corr.)
1	1.377	6.74	7.09	6.66	7.26	7.17
2	1.406	7.1	7.14	7.02	7.37	7.12
3	1.414	6.96	7.16	7.03	7.39	7.11
4	1.413	7.06	7.19	7.05	7.39	7.14
5	1.416	7.12	7.18	7.04	7.4	7.12

$$U = a\rho_0 + b, \tag{16}$$

where a and b are fitting constants, U is the C–J detonation velocity, and ρ_0 is the powder density. The density-corrected detonation velocities shown in Table 2 were found by assuming that the relationship between measured detonation velocity and charge density, specifically the slope, would be same as that shown in Eq. (16). The velocities were then corrected to the average density of the five tests and they are also shown in Table 2. The average detonation velocity for HMX corrected to an average charge density of 1.4 g/cm^3 is 7.13 km/s with a standard deviation of 27 m/s. The measurement uncertainty was found previously to be 1.68 percent, which translates to 120 m/s based on an average uncorrected detonation velocity of 7.15 km/s for HMX. The standard deviation obtained from five detonation tests appears to be lower than the measurement uncertainty.

3.3 Cocrystal Detonation Results

Images of the MDNT/CL-20 cocrystal, MDNT, and CL-20 particles are shown in Figures 4 to 6. The MDNT/CL-20 particles shown in Figure 4 have a characteristic orange color similar to those of MDNT shown in Figure 5. All three materials have fine polycrystalline particles. Particle agglomeration was also observed with all three materials.

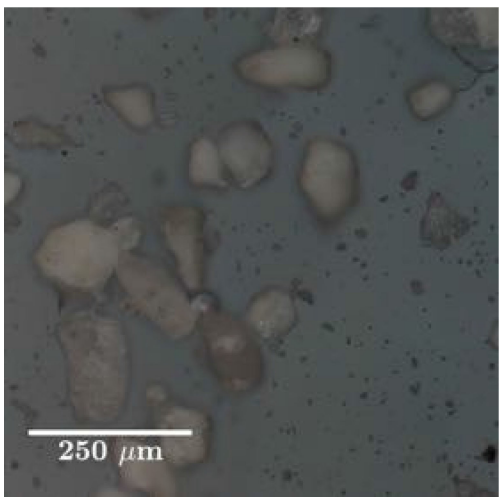

Figure 4. Microscope image of MDNT/CL-20 particles.

The cocrystal test samples were pressed to an average density of 1.398 ± 0.010 g/cm^3. The physical mix samples were pressed to an average density of 1.380 ± 0.026 g/cm^3. A measured relative permittivity for neither MDNT nor the MDNT/CL-20 cocrystal was available and due to limited availability of material, the material wavelength was determined dynamically. Four samples of each test material (cocrystal and physical mix) were prepared and detonated. An average detonation velocity for the physical mix was computed based on only three samples due to loss of data with one of the samples. Position-time plots for the cocrystal and physical mix detonation shots are shown in Figures 7 and 8.

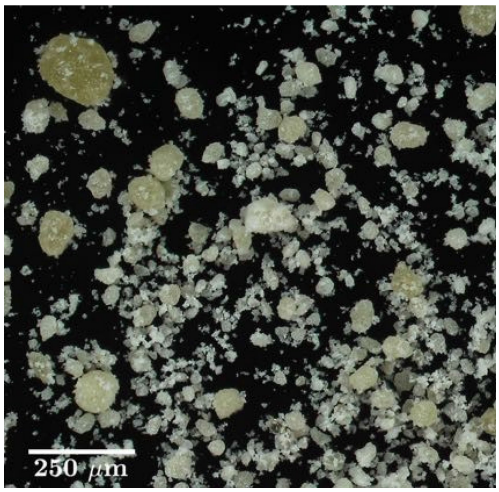

Figure 5. Microscope image of MDNT particles.

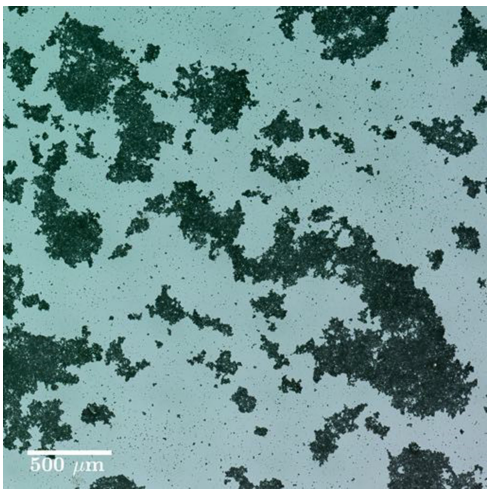

Figure 6. Microscope image of CL-20 particles.

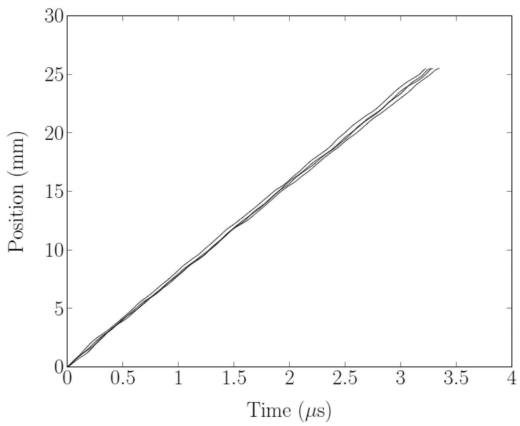

Figure 7. Position vs. time plots for MDNT/CL-20 Cocrystal detonation test.

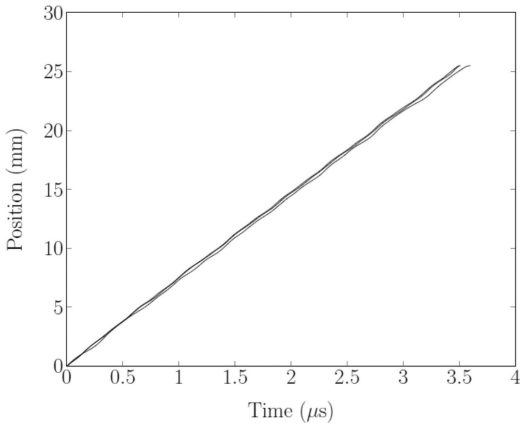

Figure 8. Position vs. time plots for MDNT/CL-20 Physical Mix detonation tests.

It can be seen in Figures 7 and 8 that similar to what was seen in Figure 3, the detonation wave was steady over the entire length of the charge for all tests. Furthermore, the position-time curves are nearly indistinguishable from one another, illustrating low shot-to-shot variation in detonation velocity. A linear- curve fit was applied to the plots shown above. The average detonation velocity for the MDNT/CL-20 cocrystal at an average charge density of $1.395 \pm .009$ g/cm^3 was measured to be 7.76 ± 0.113 km/s. The average detonation velocity corrected to a density of 1.4 g/cm^3 for the cocrystal was 7.78 ± 0.113 km/s. The average detonation velocity for the physical mix at an average charge density of 1.38 ± 0.026 g/cm^3 was measured to be 7.21 ± 0.051 km/s. The detonation velocity of the physical mixture corrected to a density of 1.4 g/cm^3 was 7.28 ± 0.044 km/s. For comparison, the measured detonation velocities of HMX, MDNT/CL-20 cocrystal, and MDNT/CL-20 physical mix corrected to a powder density of 1.4 g/cm^3 are shown in Figure 9.

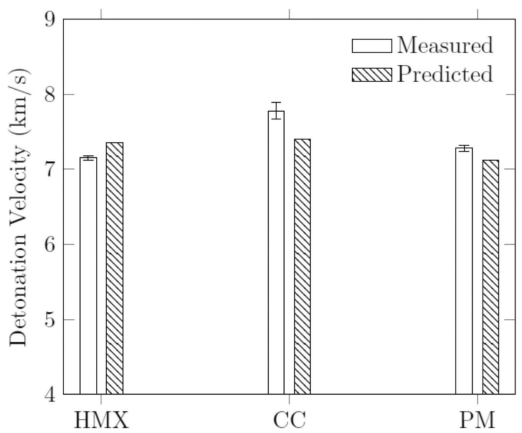

Figure 9. Measured detonation velocities for HMX, MDNT/CL-20 cocrystal, and MDNT/CL-20 physical mix (corrected to 1.4 g/cm^3).

3.4 Statistical Analysis

The observed difference between the cocrystal and physical mix is much greater than the measurement uncertainty. However, a key aspect of this experiment was to keep density constant. Analysis of variance (ANOVA) was used to determine whether a statistically significant difference in density was present among the three sets of samples. The key assumptions of the ANOVA test are that the populations being compared have equal variances and are normally distributed and that the observations within each sample are independent of each other [17].

In this case, the ANOVA test is used to test the null hypothesis that the mean detonation velocity of the cocrystal and physical mix are equal. Since there is no apparent phenomena that could result in a significantly different distribution, e. g. bimodal distribution, we assume that the detonation velocities of the cocrystal and physical mixture are normally distributed.

The cutoff value for the *F*-distribution above which the null hypothesis is rejected is [17]

$$F_c = F_{\alpha,u,v}, \tag{17}$$

where u is the degrees of freedom for the numerator defined as $u = k - 1$, where k is the number of populations being compared, v is the degrees of freedom for the denominator defined as $v = N - k$, where N is the total number of samples, and α is the level of significance also known as the complement of confidence level.

The test statistic is defined as [17]

$$F = \frac{\mathrm{MSB}}{\mathrm{MSW}}, \tag{18}$$

Where MSB is given as

$$MSB = \frac{1}{k-1}\left[\sum_{i=1}^{k}\frac{T_i^2}{n_i} - \frac{\left(\sum_{i=1}^{N} x_i\right)^2}{N}\right], \tag{19}$$

where T_i represents the sum of the values in sample i and N represents the total number of values in all of the samples. The term MSW in Eq. (18) is given as

$$MSW = \frac{1}{N-k}\left[\sum_{i=1}^{N} x_i^2 - \sum_{i=1}^{k}\frac{T_i^2}{n_i}\right]. \tag{20}$$

If the calculated value of F in Eq. (17) is greater than F_c, the null hypothesis of means being equal is rejected. The sample densities and detonation velocities are shown below in Table 3.

Using Equations 18, 19, and 20, the value of F is found to be 2.08, which is less than the critical value of 4.26 [17]. Therefore, there is no statistically significant difference in charge density among the three materials tested. This indicates that differences in detonation velocity between different materials presented in this study are not attributable to density variations.

Table 3. Charge densities.

Sample	ρ_0 (g/cm^3)	U (km/s) (Unc.)	(Corr.)
HMX-1	1.377	7.09	7.18
HMX-2	1.406	7.14	7.12
HMX-3	1.414	7.16	7.11
HMX-4	1.413	7.19	7.14
HMX-5	1.416	7.18	7.12
CC-1	1.383	7.8	7.86
CC-2	1.401	7.79	7.79
CC-3	1.402	7.86	7.85
CC-4	1.395	7.6	7.62
PM-1	1.39	7.27	7.26
PM-2	1.399	7.29	7.25
PM-3	1.35	7.08	7.33

Having established that no statistically difference in density exists among all samples tested, the same analysis was performed on the cocrystal and physical mix detonation velocity. The value of F for the uncorrected cocrystal and physical mix detonation velocities was calculated using Eq. (18) to be 39.81 and the same value for the corrected detonation velocities was 52.52. This is consistent with our observation of decreased variances in detonation velocities for the cocrystal and physical mix after correcting to 1.4 g/cm^3. Both values are much greater than the critical value of 6.61 [17]. We can therefore conclude from the *F*-test that there is a statistically significant difference in detonation velocity between the MDNT/CL-20 cocrystal and physical mixture at a charge density of about 1.4 g/cm^3.

3.5 Discussion

The required inputs to create a new reactant in CHEETAH are the crystal density, chemical formula, and enthalpy of formation. The enthalpy of formation was measured by bomb calorimetry using a Parr Instruments Calorimetric Thermometer 6772 and Semimicro Calorimeter 6725 with a 1109A Semi- Micro Oxygen Bomb (30 atm, Oxygen). The enthalpy of formation for the MDNT/CL-20 cocrystal was measured to be 1025.19 ± 147.23 kJ/mol. The enthalpy of formation for CL-20 is 377 kJ/mol [18] and the enthalpy of formation of MDNT is 122.8 kJ/mol. The calculated mixture enthalpy of formation for a 1 : 1 MDNT/CL-20 physical mixture is therefore 499.8 kJ/mol, much smaller than the measured enthalpy of formation of the MDNT/CL-20 cocrystal. This indicates that there will be a difference in detonation velocity of the cocrystal and physical mixture even at the same powder density. The crystal density was determined using X-ray diffraction [5]. The chemical formula was taken

to be the sum of all the constituent elements of the two coformers in the cocrystal.

Using the JCZ3 equation of state (EOS), it was calculated that the cocrystal would detonate about 230 m/s faster than the physical mix at a charge density of 1.4 g/cm^3. Instead, we found that the cocrystal detonation velocity was more than 500 m/s faster than that of the physical mix. As noted above, one would expect the predicted velocity to be higher than the measured velocity but we believe the difference is attributable to the EOS not performing as well as for the cocrystal as it did for HMX. However, it should still be noted that CHEETAH predicted a higher detonation velocity for the cocrystal which is what was observed for the measured detonation velocity and that, again, the predicted difference in detonation velocity between cocrystal and physical mix is greater than the estimated measurement uncertainty.

Since a cocrystal is a combination of two coformers with complementary bonding, if powder density is held constant, one would not expect there to be a significant difference in detonation velocity between the cocrystal and a physical mixture of the two coformers in the same molar ratio as contained in the cocrystal. It is known that polymorphism gives rise to multiple crystal configurations of the same crystalline material and each of these polymorphs can exhibit different properties. We know that crystalline explosives such as HMX have a number of polymorphs whose differences in crystal density and enthalpy of formation result in differences in detonation velocity among the polymorphs.

CL-20 has four polymorphs that exist at ambient conditions and/or in hydrated form (α, ε, β, γ) and a fifth polymorph known as the ζ polymorph that is theorized to exist at high pressure [19, 20]. All of these polymorphs have different crystal densities. We also note that the β and ε polymorphs have different measured enthalpies of formation, which will result in a difference in detonation velocity even if the powder density is held constant [18]. A comparison of the β and ε polymorph detonation velocities at the respective TMDs of the two polymorphs and at 1.4 g/cm^3 is shown in Figure 10 using enthalpy of formation data from Simpson et al [18]. The crystal densities of the εand β polymorphs of CL-20 are 2.044 and 1.985 g/cm^3, respectively [20].

For the ε and β polymorphs of CL-20, we calculate that at a fixed powder density of 1.4 g/cm^3, the β polymorph detonates 21 m/s faster than the ε polymorph and at full density, we calculate that the ε polymorph detonates 187 m/s faster. This calculation shows that changes in the crystal structure can alter the properties of the material. In a cocrystal, the coformers are arranged such that a unique crystal structure results. The difference observed in detonation velocity between the physical mixture and cocrystal is therefore attributable to the contribution of bonding energy and crystal structure that results from cocrystallization. In this case, the difference between the cocrystal and physical mix was larger at a powder density of 1.4 g/cm^3, both measured and predicted. However, it can be seen in Figure 11 that at their respective TMD, the cocrystal and physical mix detonate at almost the same velocity, with the difference being about 20 m/s. This prediction implies that with the MDNT/CL-20 cocrystal, the advantage in detonation performance from the changed crystal structure of the cocrystal decrease as the powder densities of the cocrystal and physical mix approach their respective TMD.

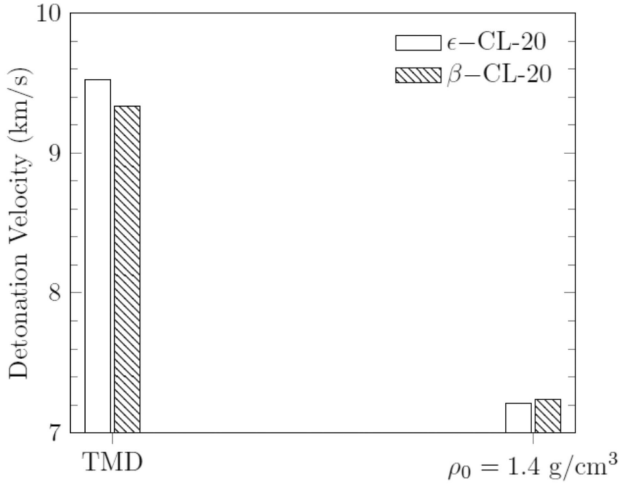

Figure 10. Detonation velocities of β and ε polymorphs of CL-20.

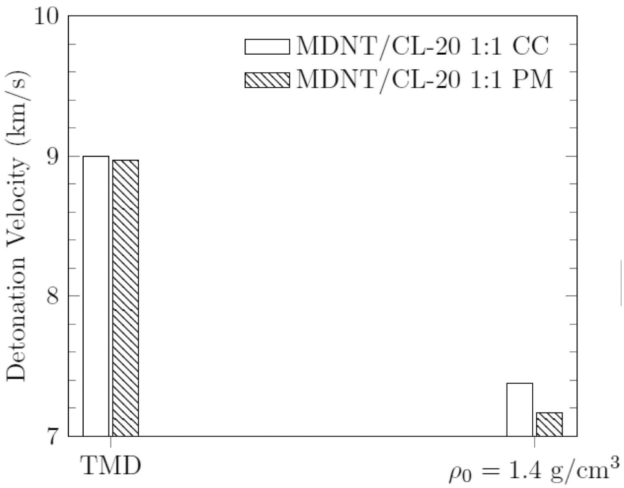

Figure 11. Predicted detonation velocities of MDNT/CL-20 cocrystal and physical mixture.

As noted previously, an unexpected result was that the cocrystal and physical mix had measured detonation velocities higher than what was predicted with CHEETAH, although the difference between measured and predicted detonation velocity for the physical mixture was well below

the measurement uncertainty and the observed standard deviation. The under-predicted detonation velocity by CHEETAH is unexpected because CHEETAH calculates the Chapman-Jouguet detonation velocity, which assumes infinitesimal reaction zone thickness. This assumption would be most valid for an ideal explosive at infinite charge diameter. For this reason, it would normally be expected that the observed detonation velocity in this study would be lower than what is predicted by CHEETAH, as it is for HMX for example. However, the measured detonation velocity for RX-39-AA, a PBX consisting of 95.8 percent CL-20 and 4.2 percent Estane binder was found to be 200 m/s faster than what was predicted by CHEETAH using the JCZ3 equation of state [18]. We believe that this is attributable to EOS weakness in predicting the final state of products.

4 Conclusion

It has been demonstrated in this work that with less than 1.5 g per sample, microwave interferometry can be used to resolve detonation velocity differences as small as 100 m/s or less. This was achievable largely due to tight control of sample-to-sample variation in charge density and precise hardware used. With HMX, velocity variations below 50 m/s were obtained. It has also been demonstrated that with an ideal explosive, appropriate matching of density between the booster and sample charge can yield a steady detonation wave propagating over essentially the entire length of the sample charge, making it possible to determine the steady detonation velocity of the sample. This method was then applied to measure the steady detonation velocity of a cocrystal of MDNT and CL-20. It was found in this study that at a density of about 1.4 g/cm^3, the MDNT/CL-20 1 : 1 cocrystal detonates over 500 m/s faster than the MDNT/CL-20 1 : 1 physical mix at the same charge density.

Since no previous work has been reported on detonation performance characterization of the MDNT/CL-20 cocrystal this work yields insights into the detonation performance of the MDNT/CL-20 cocrystal, which is important in evaluating its feasibility for scale-up. The experimental method presented in this work demonstrates a method for evaluating detonation performance of materials available in limited supply. This work also examines the contribution of coformer bonding within the cocrystal to detonation performance. The observed difference in detonation velocity between the cocrystal and physical mix indicates that the crystal structure and resulting coformer bond energy contribute to the observed difference in detonation velocity between the cocrystal and physical mix.

Acknowledgements

This material is based upon work supported by the U.S. Army Research Laboratory and the U.S. Army Research Office under contract/grant number W911NF-13-1-0387. This paper is dedicated to the memory of Dr. Michael Hiskey for this special edition. Being able to study some of the new molecules Mike made when we were both at Los Alamos is such a great memory. We had more fun than anyone really should at work. More importantly, was his kind heart. Mike and I (SFS) published more than 20 papers together, and he always kept it "real".

References

[1] T. Friščić, W. Jones, Benefits of cocrystallisation in pharmaceutical materials science: an update, *J. Pharm. Pharmacol.* **2010**, *62*, 1547–1559.
[2] O. Bolton, A. J. Matzger, Improved stability and smart-material functionality realized in an energetic cocrystal, *Angewandte Chemie Int. Ed.* **2011**, *50*, 8960–8963.
[3] O. Bolton, L. R. Simke, P. F. Pagoria, A. J. Matzger, High Power Explosive with Good Sensitivity: A 2 : 1 Cocrystal of CL-20:HMX, *Cryst. Growth & Des.* **2012**, *12*, 4311–4314.
[4] P. Ravi, D. M. Badgujar, G. M. Gore, S. P. Tewari, A. K. Sikder, Review on melt cast explosives, *Propellants, Explos. Pyrotech.* **2011**, *36*, 393–403.
[5] S. R. Anderson, P. Dubé, M. Krawiec, J. S. Salan, D. J. am Ende, P Samuels, Promising CL-20-based energetic material by cocrystallization, *Propellants, Explos. Pyrotech.* **2016**, *41*, 783–788.
[6] S. R. Anderson, D. J. am Ende, J. S. Salan, P. Samuels, Preparation of an energetic-energetic cocrystal using resonant acoustic mixing, *Propellants, Explos. Pyrotech.* **2014**, *39*, 637–640.
[7] G. F. Cawsey, J. L. Farrands, S. Thomas, Observations of Detonation in Solid Explosives by Microwave Interferometry, *Proc. Royal Soc. A: Math. Phys. Eng. Sci.* **1958**, *248*, 499–521.
[8] A. D. Krall, B. C. Glancy, H. W. Sandusky, Microwave interferometry of shock waves. I. Unreacting porous media, *J. Appl. Phys.* **1993**, *74*, 6322–6327.
[9] B. C. Glancy, H. W. Sandusky, A. D. Krall, Microwave interferometry of shock waves. II. Reacting porous media, *J. Appl. Phys.* **1993**, *74*, 6328–6334.
[10] N. J. Burnside, S. F. Son, B. W. Asay, P. M. Dickson, Deflagration to detonation experiments in granular hmx. Technical Report LA-UR-97-4312; CONF-9710108, Los Alamos National Lab., NM (United States), **1998**.
[11] J. W. Tringe, R. J. Kane, K. S. Vandersall, F. Garcia Converse, F. Gar- cia, C. M. Tarver, Microwave Interferometry for Understanding Deflagration-to-Detonation and Shock-to-Detonation Transitions in Porous Explosives. Technical report, Lawrence Livermore National Laboratory (LLNL), Livermore, CA, **2014**.
[12] R. S. Janesheski, L. J. Groven, S. F. Son, Detonation failure characterization of homemade explosives, *Propellants, Explos. Pyrotech.* **2014**, *39*, 609–616.
[13] D. E. Kittell, N. R. Cummock, S. F. Son, Reactive flow modeling of small scale detonation failure experiments for a baseline non-ideal explosive, *J. Appl. Phys.* **2016**, *120*, 064901.
[14] D. E. Kittell, J. O. Mares, S. F. Son, Using time-frequency analysis to determine time-resolved detonation velocity with microwave interferometry, *Rev. Sci. Instruments* **2015**, *86*, 044705.
[15] G. H. McCall, W. L. Bongianni, G. A. Miranda, Microwave interferometer for shock wave, detonation, and material motion measurements, *Rev. Sci. Instruments* **1985**, *56*, 1612–1618.
[16] D. E. Kittell, Analysis and Simulation of Small-Scale Microwave Interferometer Experiments on Non-Ideal Explosives. PhD thesis, Purdue Univ., **2016**.

[17] R. V. Dukkipati, *Probability and statistics for scientists and engineers*, New Academic Science Limited, **2013**.
[18] R. L. Simpson, P. A. Urtiew, D. L. Ornellas, G. L. Moody, K. J. Scribner, D. M. Hoffman, CL-20 performance exceeds that of HMX and its sensitivity is moderate, *Propellants, Explos. Pyrotech.* **1997**, *22*, 249–255.
[19] J. Ciezak, T. Jenkins, Z. Liu, Evidence for a high-pressure phase transition of −2,4,6,8,10,12-hexanitrohexaazaisowurtzitane (CL-20) using vibrational spectroscopy, *Propellants, Explos. Pyrotech.* **1997**, *32*, 472–477.
[20] A. T. Nielsen, A. P. Chafin, S. L. Christian, D. W. Moore, M. P. Nadler, R. A. Nissan, D. J. Vanderah, R. D. Gilardi, C. F. George, J. L. Flippen-Anderson, Synthesis of polyazapolycyclic caged polynitramines, *Tetrahedron* **1998**, *54*, 11793–11812.

Received: June 3, 2017
Published online: August 7, 2017

